

# RSC Advances



This is an *Accepted Manuscript*, which has been through the Royal Society of Chemistry peer review process and has been accepted for publication.

*Accepted Manuscripts* are published online shortly after acceptance, before technical editing, formatting and proof reading. Using this free service, authors can make their results available to the community, in citable form, before we publish the edited article. This *Accepted Manuscript* will be replaced by the edited, formatted and paginated article as soon as this is available.

You can find more information about *Accepted Manuscripts* in the [Information for Authors](#).

Please note that technical editing may introduce minor changes to the text and/or graphics, which may alter content. The journal's standard [Terms & Conditions](#) and the [Ethical guidelines](#) still apply. In no event shall the Royal Society of Chemistry be held responsible for any errors or omissions in this *Accepted Manuscript* or any consequences arising from the use of any information it contains.

## pH-Responsive liquid crystal double emulsion droplets prepared using microfluidics

Jung-Yeon Kwon, Mashooq Khan, and Soo-Young Park\*

Department of Polymer Science & Engineering, Polymeric Nanomaterials Laboratory, School of Applied Chemical Engineering, Kyungpook National University, #1370 Sangyuk-dong, Buk-gu, Daegu 702-701, Korea

\*Corresponding author email: psy@knu.ac.kr

**Abstract:** Functionalized nematic liquid crystal (NLC) double emulsion droplets (DEDs) with different anchoring conditions on the inner and outer NLC surfaces were produced using a microfluidic method that employed glass capillaries with a combined co-flow and flow-focusing geometry. Planar (P) and homeotropic (H) NLC DED configurations were achieved using poly(vinyl alcohol) (PVA) and a mixture of sodium dodecyl sulfate (SDS)/Polysorbate 80 (TWEEN 80), respectively. The H configuration was not stable using SDS alone, and required the use of a mixture of SDS and TWEEN 80. The P/P, P/H, H/P, and H/H configurations on the inner/outer surfaces exhibited different defect structures, as predicted by the Poincaré theorem. The transition from the P to H configuration on the outer surface was monitored by replacing the PVA aqueous solution (used to give initial P configurations on both the inner and outer surfaces) with the aqueous SDS/TWEEN 80 solution. The defect structures located on top of the NLC DED had a total defect strength of 2 and the defects were positioned at opposite poles during the P-to-H transition. The outer configuration of the poly(acrylic acid) (PAA)-coated NLC DED (NLC DED<sub>PAA</sub>) was pH-responsive, with P and H configurations observed below and above the pK<sub>a</sub> of PAA, respectively. In addition, NLC DED<sub>PAA</sub> was utilized for glucose detection by monitoring changes in the defect structures, which were brought about by a decrease in pH during an enzymatic reaction of glucose. A systematic study on the defect structure in NLC DEDs is of paramount importance for the liquid crystals field. In this work, we reported a method of preparing pH-responsive NLC DEDs, which can be used as a new biosensor platform by detecting these unique defect structure.

**Keywords:** Liquid crystal, microfluidics, double emulsion, defect, biosensor.

## Introduction

Nematic liquid crystal (NLC) single-emulsion droplets (SEDs) have been developed, using microfluidic methods, for biosensor applications by decorating their surfaces with materials capable of changing the NLC surface anchoring orientation from parallel to perpendicular (or vice versa) in response to environmental changes, such as variations in pH,<sup>1</sup> binding with proteins,<sup>2-4</sup> and enzymatic reactions.<sup>5</sup> The coating materials can be surfactants,<sup>6</sup> polyelectrolytes,<sup>7, 8</sup> or pH-sensitive block copolymers.<sup>9, 10</sup> NLC SEDs with parallel (planar, P) and perpendicular (homeotropic, H) anchoring configurations are also known as bipolar and radial droplets, respectively. Bipolar and radial NLC SEDs are typically produced by coating their liquid crystal (LC) surfaces with poly(vinyl alcohol) (PVA) and sodium dodecyl sulfate (SDS), respectively.<sup>11</sup> NLC SEDs can also be functionalized using polyelectrolyte-*b*-SGLCP (SGLCP: side group LC polymer) block copolymers, where the polyelectrolyte block is in a charged state and the SGLCP block anchors the LC at the LC/aqueous interface.<sup>10</sup> The use of strong polyelectrolytes, such as poly(sodium styrene sulfonate) (PSS)<sup>7, 12</sup> and quaternized poly(4-vinylpyridine) (QP4VP),<sup>13</sup> induced the H configuration in NLC SEDs regardless of pH, whereas weak polyelectrolytes, such as poly((dimethylamino)ethyl methacrylate) (PDMAEDA)<sup>14</sup> and poly(acrylic acid) (PAA),<sup>1</sup> induced either the H or P configuration depending on the pH of the aqueous solution. For example, PAA-*b*-LCP (LCP: poly(4-cyanobiphenyl-4'-oxyundecylacrylate)) was found to be an effective coating material that allowed alteration of the NLC SED configuration by pH variation through protonation/deprotonation of the PAA carboxyl group.<sup>1</sup> At high pH values, the charged PAA state induced the H configuration through deprotonation, while at low pH values the neutral PAA state induced the P configuration through protonation at the LC/aqueous interface. Notably, using PAA-*b*-LCP to coat the NLC SED surfaces allowed easy coupling with other ligands possessing amine groups via a 1-ethyl-3-(3-dimethylaminopropyl)carbodiimide/*N*-hydroxysuccinimide/1-ethyl-3-(3-dimethylaminopropyl)carbodiimide (EDC-NHS) coupling reaction. Several enzymes such as glucose oxidase (GOx), cholesterol oxidase (ChO), and urease have been coupled on the surface of the PAA-decorated NLC SED for the detection of glucose,<sup>15</sup> cholesterol,<sup>16</sup> and urea,<sup>17</sup> respectively. These NLC SED biosensors are unique because they allow detection of biomaterials through changes in optical appearance using optical microscopy without requiring sophisticated instruments or labeling.

NLC double-emulsion droplets (DEDs) are an alternative platform for biosensor applications. NLC DEDs can be composed of water-filled cores within NLC shells. When the core is filled with water, both the inner and outer surfaces of the NLC DEDs can be exposed to water. As the NLC can be anchored in the H or P configuration against each surface, four different configurations (H/H, H/P, P/H, and P/P, at the outer/inner surfaces) are possible depending on the anchoring conditions at each NLC DED interface. According to the Poincaré theorem, when a flat NLC surface with a P configuration forms an NLC shell, defect structures appear on the surface, with a total defect strength (*s*) of 2.<sup>18</sup> The total defect strength can be divided into two

+1 defects (a bipolar droplet), one +1 and two +1/2 defects, or four +1/2 defects, each of which gives different NLC DED defect structures and different brush shapes when observed through a polarized optical microscope (POM) under crossed polarizers.<sup>19</sup> However, when the NLC DED surface is in the H configuration, no defect structures are observed. Thus, if the NLC DED surface is decorated with materials that promote a P to H configurational change (or vice versa) at the surface in response to environmental variations (e.g., pH changes, protein adsorption, or enzymatic reactions), the NLC DED can be employed as a biosensor by observing changes in the defect structure using POM.

We herein report the use of PAA-*b*-LCP-decorated NLC DEDs (NLC DED<sub>PAA</sub>) as pH-responsive NLC DEDs. The NLC DED defect structure changed with pH, based on the pK<sub>a</sub> value of PAA, and the GOx-immobilized NLC DED<sub>PAA</sub> (NLC DED<sub>PAA-GOx</sub>) successfully detected small amounts of glucose, demonstrating that NLC defect configurational changes can potentially be used in biosensor applications.

## Experimental

**Materials:** 4-Cyano-4'-pentylbiphenyl (5CB) (purity 99.5%, Qingdao QY Liquid Crystal Co., Ltd., China), polyvinyl alcohol (PVA) (Yakuri, Japan), sodium dodecyl sulfate (SDS) (DC Chemical Co., Ltd., South Korea), polysorbate 80 (Sigma Aldrich, USA), rhodamine 6G (Sigma Aldrich, USA), D-(+)-glucose (Sigma Aldrich, USA), *N*-hydroxysuccinimide (NHS) (Sigma Aldrich, USA), glucose oxidase (GOx, E.C. 1.1.3.4) from *Aspergillus niger* (Sigma Aldrich, USA), *N*-(3-dimethylaminopropyl)-*N'*-ethylcarbodiimide hydrochloride (EDC·HCl) (Sigma Aldrich, USA), and pH buffer solutions (Samchun Pure Chemical, South Korea) were all used as received. A solution of 2 wt% (3-aminopropyl)triethoxysilane (APTES) (TCI, Japan) in ethanol was used to prepare the hydrophilic coatings, and a solution of 2 wt% octadecyltrichlorosilane (OTS) (TCI, Japan) in toluene was used to prepare the hydrophobic coatings. A square capillary tube (Vitrocom, USA, 0.9 mm × 0.9 mm) was used as received without any surface treatment. Round glass capillary tubes (Vitrocom, USA, 0.7 mm inner diameter × 0.87 mm outer diameter × 100 mm length) were tapered at the halfway point using a Micropipette Puller (P-97, Sutter Instrument Co., USA) and hydroxylated with hot piranha solution (H<sub>2</sub>O<sub>2</sub> (35%):H<sub>2</sub>SO<sub>4</sub> (98%) = 1:1 (v/v)) for 30 min; they were then washed with water and dried under nitrogen gas. It should be noted that piranha solution is extremely corrosive and must be handled with extreme care. Polymerization to give PAA(22k)-*b*-LCP(6k) was carried out using a previously reported method (see Scheme S1).<sup>10</sup>

**Preparation of NLC DED<sub>PAA</sub>:** A micro-capillary device consisting of round glass capillary tubes enclosed within a square glass tube was used to prepare the NLC DEDs.<sup>20</sup> The outer diameter of the round capillaries (0.87 mm) was comparable to the inner diameter of the square capillary (0.9 mm), such that a round capillary could be inserted into the square capillary from each end to achieve tight-fitting coaxial alignment. The diameters of the left and right capillaries

were  $120\pm 10\ \mu\text{m}$  and  $270\pm 20\ \mu\text{m}$ , respectively, with the tapered ends of the two capillaries facing each other at the center of the square capillary, as shown in Figure 1b. For the preparation of NLC DEDs, the inner aqueous phase flowed through the left capillary, while the LC flowed along the same direction in the square capillary; the outer continuous aqueous phase flowed in the opposite direction. Droplets of the inner aqueous phase formed within the LC phase, as Rayleigh instability broke up the stream of the two co-flowing fluids. The LC and continuous aqueous phases met between the ends of the two round capillaries, and because of their immiscibility, the resulting DEDs were dispersed into the right-hand capillary, which acted as a collection tube. Flow rates were controlled using a pneumatic microfluidic flow rate control system (MFCS-EZ, Flow-Rate Platform and Flow-Rate Control Module, Fluigent, France) capable of pumping three fluids at a specified velocity. These systems were connected to the microcapillary device using shrinkable connector tubes (diameters = 1.5, 2, and 3 mm) and flexible plastic tubing (Norton, USA, 0.51 mm inner diameter, 1.52 mm outer diameter). By pumping nitrogen gas into the Fluiwell (Fluigent, France) containing the liquids at a finely controlled rate, the MFCS-EZ unit was used to pressurize the Fluiwell, such that fluids began to flow through the tubes and into the device. To stabilize the shells and prevent them from rupturing, the two aqueous phases must contain either a surfactant or polymer that adsorbs at the LC/aqueous interface.<sup>21</sup> We selected PVA, SDS, TWEEN 80, and PAA-*b*-LCP for use in this study. The stability of the resulting NLC DEDs will be discussed later. The typical flow rates used for NLC DED formation were 12, 60, and 850 mL/min for the inner aqueous, dispersed LC, and continuous aqueous phases, respectively. The NLC DEDs produced were collected in a vial at the end of the outlet tubing and examined by POM under crossed polarizers using a CCD camera.

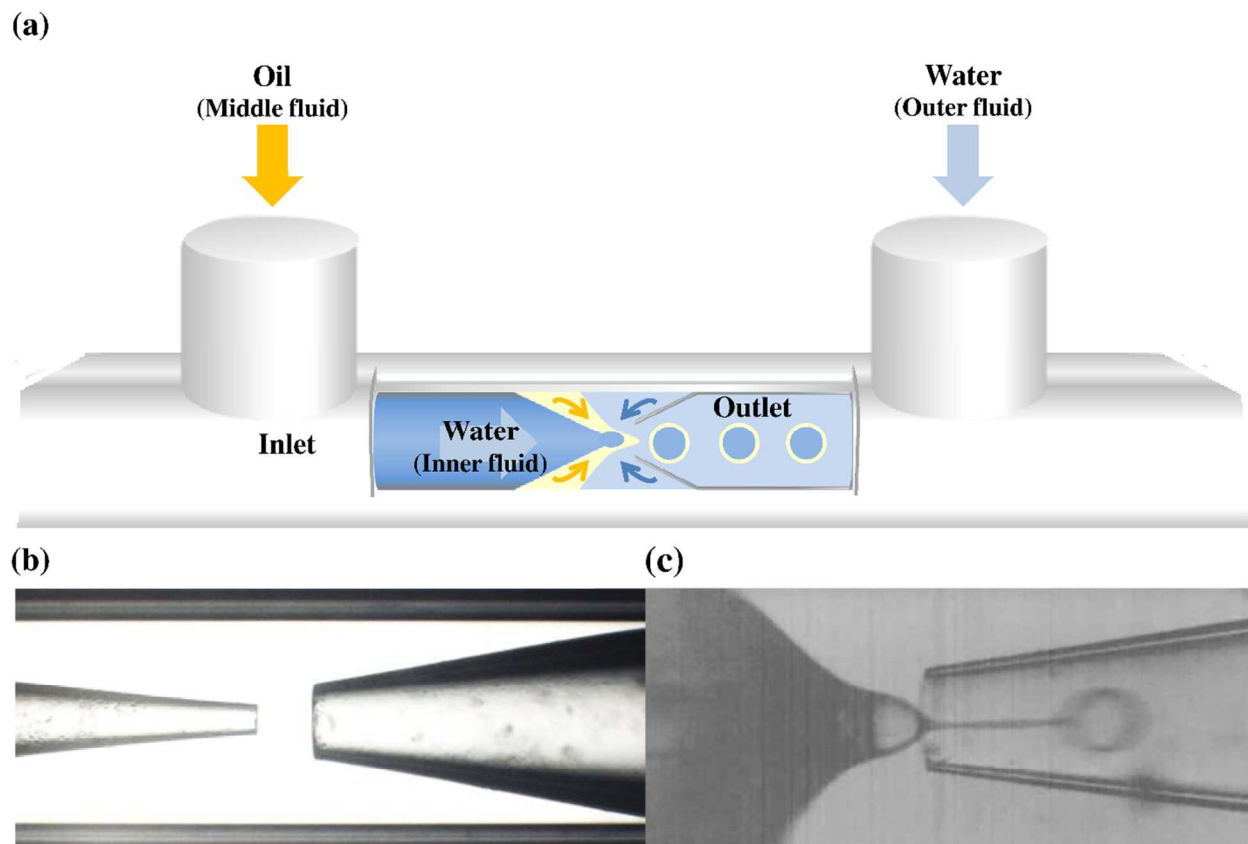


**Figure 1.** (a) Schematic of the capillary microfluidic device combining co-flow and flow-focusing geometries. Photographic images of the microfluidic capillary devices used in the (b) absence and (c) presence of fluids.

**GOx-immobilized LC double emulsion droplet:** The collected NLC DED<sub>PAA</sub>S were activated in a vial using EDC·HCl:NHS (0.4 M:0.1 M) in phosphate-buffered saline (PBS, pH 7.0) for 1 h. The NLC DED<sub>PAA</sub>S were then placed in GOx solution (19 μM) at 20 °C for 12 h to obtain the GOx-immobilized NLC DEDs (NLC DED<sub>GOx</sub>). The immobilization of GOx on the PAA was confirmed using GOx labeled with rhodamine 6G (GOx<sub>-rhd</sub>), which was prepared as follows: GOx was dissolved in PBS (pH 7.0) in a reaction vial to give a 15.6 μM solution into which EDC·HCl (0.4 M) and NHS (0.1 M) were added; the vial was allowed to stand for 1 h to activate the GOx carboxyl groups (-COOH). Rhodamine 6G (1 mg) was then added to the solution and the mixture was stirred at 20 °C for 12 h. The resulting GOx<sub>-rhd</sub> was immobilized on the NLC DED<sub>PAA</sub> using the previously described method. Following immobilization, the solution was diluted with distilled water to remove unreacted GOx<sub>-rhd</sub>, and the resulting GOx<sub>-rhd</sub>-immobilized NLC DED<sub>PAA</sub>S (NLC DED<sub>GOx-rhd</sub>) were examined by fluorescence microscopy.

**Measurements:** The formation of NLC DEDs on a chip was imaged using an inverted

microscope (JSP-20T, Samwon, South Korea) equipped with a high-speed recording camera (Motion BLIZT Cube4, Mikroton, Germany). The resulting NLC DEDs were examined using a POM (ANA-006, Leitz, Germany), under crossed polarizers, equipped with a CCD camera (STC-TC83USB, Samwon, South Korea). GOx<sub>rhd</sub> was analyzed by UV-Vis spectrometry (UV-2401PC, Shimadzu, Japan), and the presence of GOx<sub>rhd</sub> on the NLC DED<sub>PAAAS</sub> was confirmed using fluorescence microscopy (E600POL, Nikon Eclipse, Japan).

## Results and discussion

**Preparation of NLC DEDs:** Figure 1a presents a schematic representation of the capillary microfluidic device used for combining the co-flow and flow-focusing geometries in the preparation of NLC DEDs. As shown on the left-hand side of Figure 1a, the inner fluid (water + stabilizing materials) was pumped through the tapered circular capillary, while the middle fluid (5CB), which was immiscible with the aqueous inner and outer fluids, flowed through the outer square capillary in the same direction. PVA, SDS, TWEEN 80, and PAA-*b*-LCP were used to stabilize the droplets, and will be discussed further in the next section. Figures 1b and c show photographic images of the microfluidic capillary device in the absence and presence of fluids, respectively. In addition, Video S1 in the Supporting Information shows the stable production of mono-dispersed NLC DEDs. The size and wall thickness of the NLC DEDs were controlled by varying  $Q_i$ ,  $Q_m$ , and  $Q_o$ , which represent the inner, middle, and outer flow rates, respectively. We observed a stable dripping regime for NLC DED production when  $Q_i = 60 \pm 2.1$ ,  $Q_m = 12 \pm 0.8$ , and  $Q_o = 850 \pm 5.3$   $\mu\text{L}/\text{min}$ , resulting in an NLC DED outer diameter of  $223.2 \pm 3.4$   $\mu\text{m}$  and a wall thickness of  $9.4 \pm 2$   $\mu\text{m}$ . It should, however, be noted that some variation of fluid flow occurred in these dimensions due to unavoidable differences in the size of the tapered ends of the round capillaries. These flow rates were used to produce all the NLC DEDs discussed herein, unless otherwise stated.

**Functionalization of NLC DEDs with SDS and PVA:** Stabilizing materials were added to the water to provide long-term stability for the produced NLC DEDs, and to control the anchoring mode at the NLC/aqueous interface. PVA is the most frequently used stabilizing material for NLC SED formation, and yields the P configuration at the NLC/aqueous interface. PVA is a nonionic and polar polymer that leads to planar orientation. Because of the polar nature of PVA, it may strongly wrap the LC droplets, which have a high dipole moment, leading to an increase in droplet stability. Another reason for the high stability may be the orientation of the long mesogenic groups. The long axis is parallel to the surface for planar orientation and perpendicular for homeotropic orientation; therefore, the integrity of a liquid crystal having planar orientation may be higher than that of a crystal having homeotropic orientation, because the contact area with water per LC molecule is higher for planar orientation. Figure 2a presents

the POM images of the NLC DEDs when both the inner and outer fluids consisted of 1 wt% PVA aqueous solution. The PVA solution ensured the long-term stability of the DEDs and gave P boundary conditions at both surfaces. Four defects with  $s = +1/2$  (the number of brushes is two at the defect; the defects are characterized by the number of black brushes ( $4|s|$ )) were observed on top of the droplet. Other defect structures with defect strengths of two  $+1$ s, one  $+1$ , and two  $+1/2$ s were also observed on top of the droplet, as shown in Figure S1. The P boundary conditions led to a defect structure characterized by two pairs of half-hedgehogs separated at the poles of each surface for a thick shell ( $a \leq R/2$ , where  $a$  is the thickness of shell and  $R$  is the outer radius of the shell).<sup>22</sup> In contrast, three types of defect structures (distinguished by the number and type of defects, i.e., four  $+1/2$ s, two  $+1/2$ s and one  $+1$ , and two  $+1$ s) were observed on top of the NLC DEDs for a thin shell ( $a \geq R/2$ ).<sup>19</sup> These defects in the thin shells were all located on top of the drops, due to buoyancy forces caused by the density difference between 5CB and the inner water drop. According to the Poincaré theorem, these defects should exist on both the inner and outer surfaces. However, due to the presence of the shell, only the defect pair on the outer surface was observed; therefore, according to the Poincaré theorem, a second pair must exist below this pair, which requires a total topological charge of  $s = +2$  on both surfaces. Thus, the defect structures observed for the thin NLC DEDs ( $R = 223.2 \pm 3.4 \mu\text{m}$  and  $a = 9.4 \pm 2 \mu\text{m}$ ) produced using a 1 wt% aqueous PVA solution in both the inner and outer fluids were in agreement with those reported in the literature.

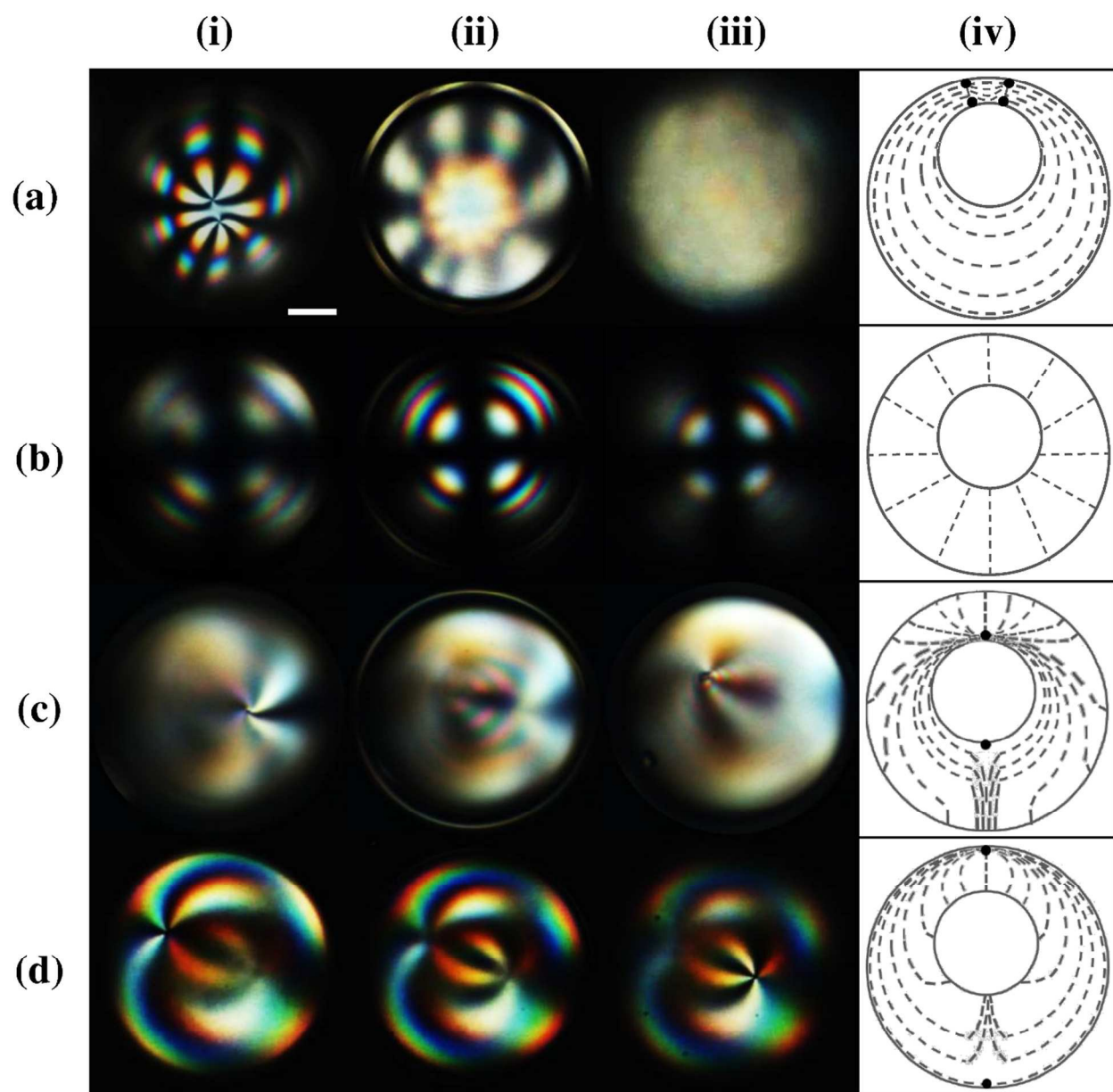


**Figure 2.** POM images and direct field diagrams for functionalized NLC DEDs with four different configurations: (a) P/P, (b) H/H, (c) P/H, and (d) H/P (inner/outer), with the focal planes of the microscope at the (i) top, (ii) middle, and (iii) bottom of the NLC DED. Column (iv) shows the direct field diagrams for each configuration. The P and H configurations were obtained using aqueous 1 wt% PVA and 1 wt% SDS/TWEEN 80 solutions, respectively. The scale bar is 50  $\mu\text{m}$ .

SDS was also used as a stabilizing material to promote H orientation at the NLC/aqueous interface. With the director perpendicular to the NLC SED surface,  $s$  must be +1 and the defect must be contained inside the spherical volume, meaning that no defects were present on the

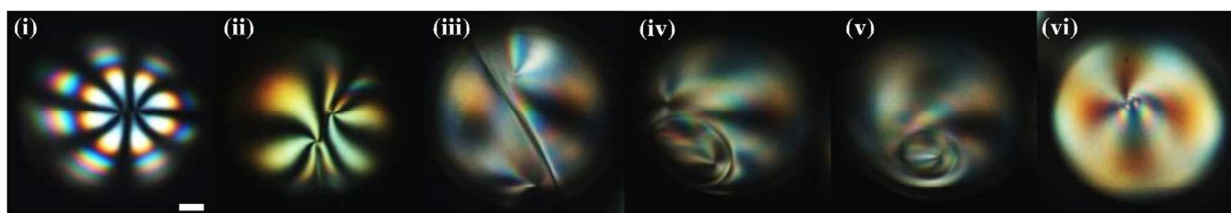
surface. When the inner and outer fluids used for NLC DED production were both 1 wt% aqueous SDS solutions, the aqueous phase ultimately enforced H boundary conditions at both surfaces. However, the resulting NLC DEDs were unstable, rupturing and forming NLC SEDs immediately following storage of the NLC DEDs in the reservoir. An SDS/TWEEN 80 mixture was then tested for its ability to allow a stable H orientation on the surface. TWEEN is a polysorbate surfactant containing a fatty acid ester moiety and a long polyoxyethylene chain, and is commonly employed as a nonionic surfactant for the preparation of stable oil-in-water emulsions.<sup>23</sup> Unless otherwise stated, for all experiments, the concentrations of both SDS and TWEEN 80 in the aqueous solution were 1 wt%, and a 50:50 wt% mixture of the two solutions was employed. Figure 2b shows the POM images of the NLC DEDs under crossed polarizers when a 1 wt% aqueous SDS/TWEEN 80 solution was employed for the inner and outer fluids. A clear Maltese-cross pattern was observed, indicating that the NLC molecules adopted the H orientation on both surfaces. The resulting NLC DEDs exhibited improved stability over those produced using only aqueous SDS solutions; thus, we conclude that the 1 wt% aqueous SDS/TWEEN 80 solution was effective for stabilization of NLC DEDs with H orientation at both NLC/aqueous interfaces.

It is also possible that the nematic director of the NLC DED can have P orientation at one surface and H orientation at the other, thus creating a hybrid shell. Figure 2c presents the POM images of an NLC DED under crossed polarizers using aqueous 1 wt% PVA and SDS/TWEEN 80 solutions as the inner and outer fluids, respectively, during NLC DED production. In addition, Figure 2d shows images of the material where the inner and outer fluids were exchanged. These hybrid shells contain two defects with  $s = +1$  (with four brushes). These defects consist of half hyperbolic and half radial hedgehogs, as observed in the direct fields in the shell in Figure 2(iv). The first defect was observed when the focus of the lens was on top of the droplet, while the second defect was observed when the focus of the lens was at the bottom of the droplet, indicating that the two defects were separated at the poles of the droplet (see top and bottom of Figures 2c and d). This defect structure is also visible when P anchoring occurs at both the inner and outer surfaces, as described for Figure 2a. The main differences between the defect structures of the all-P and hybrid configurations are in the positions of the defects and the darkness of the brushes. The defects of the NLC DED with all-P configuration were gathered on top of the droplet when the shell was sufficiently thin. However, the defects of the NLC DED with hybrid configuration were located at the poles. This separation may be due to increased repulsion between two point defects with the same charges.<sup>19, 24</sup> The increased darkness of the brush for the NLC DED with all-P configuration may be due to the overlap of brushes on both the inner and outer surfaces.

Different configurations were observed when the anchoring conditions at the inner and outer surfaces were changed, as shown in Figure 2. To apply such a system to sensors, a change in configuration should occur when the environmental conditions are altered. A typical experiment

for demonstrating a response to a stimulus involves replacing a concentrated aqueous SDS solution with an aqueous PVA solution (or vice versa) in the NLC DED container. Figure 3 shows the change in the observed POM images along with a schematic representation of the approximate positions of the point defects with respect to the disclination lines of the NLC DEDs (exhibiting an initial P/P configuration in the presence of an aqueous PVA solution at the inner and outer surfaces) over time, following the addition of a 1 wt% aqueous SDS/TWEEN 80 solution to a 1 wt% aqueous PVA solution. Although PVA was not removed from the continuous phase, the mixed solution resulted in an H orientation because of the diffusion of SDS. This process was dependent on the concentration of the solution, which controlled the time taken for the surfactant molecules to diffuse to the NLC DEDs. Initially, two +1 defects were observed on the outer surface (Figure 3a(i)); however, after H orientation anchoring had been adopted, the outer surface defects disappeared, leading to generation of a disclination line due to collisions between the director directions (Figure 3a(ii)), as previously reported.<sup>24</sup> The two initial +1 defects on the inner surface began to move away on a disclination ring, and they escaped from the disclination ring as separation increased (Figure 3a(iii)). The disclination ring containing a single defect shrank and the two defects were pulled closer together (Figure 3a(iv)). These two defects (one within the disclination ring and the other outside the ring) were then separated once more as the disclination ring shrank further (Figure 3a(v)), and were finally located at opposite poles (Figure 3a(vi)). In previous studies,<sup>24</sup> two different pathways have been proposed for this process, depending on the shell thickness. However, in our case, a slightly different scenario was observed. The main difference was that the separation between the disclination line and two defects was not large early in the process. After the disclination ring became significantly smaller (as in Figure 3a(iv)), the defects began to move away from one another (Figures 3a(v–vi)). This separation between the defects was due to repulsion, as both defects possessed the same charge. The final structure is known to be a hybrid nematic shell;<sup>24</sup> it contains two defects at the poles of the inner surface, but no defects on the outer surface.

(a)



(b)

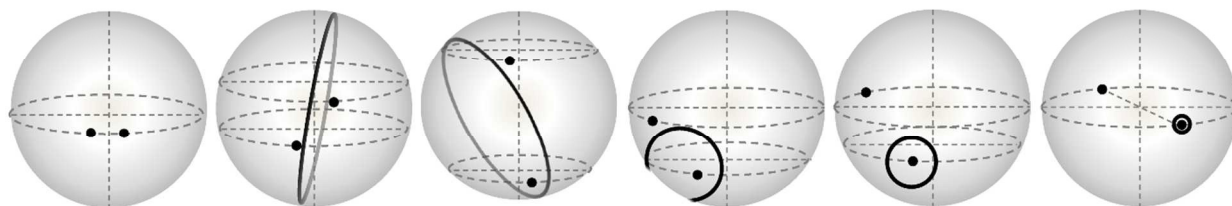


**Figure 3.** (a) Changes in the POM images of NLC DEDs with  $R = 220 \mu\text{m}$  and thickness =  $10 \mu\text{m}$  over time, following the addition of a 1 wt% aqueous SDS/TWEEN 80 solution to a 1 wt% aqueous PVA solution of the outer fluid. (b) Schematic representation of the approximate positions of point defects with respect to the disclination line. The scale bar is  $30 \mu\text{m}$ .

**Functionalization of NLC-DEDs with PAA-*b*-LCP:** The outer surfaces of the NLC DEDs were coated with PAA using a 0.2 wt% aqueous PAA-*b*-LCP solution. The NLC DED core was filled with a 1 wt% aqueous SDS/TWEEN 80 solution, as the H configuration of the inner surface improved the visibility of the NLC DEDs under POM using crossed polarizers. PAA is a weak polyelectrolyte with a  $\text{pK}_a$  of 4.26. Below this  $\text{pK}_a$ , PAA is protonated and is shrunken in its neutral state, while above this  $\text{pK}_a$ , it is deprotonated and swollen due to its negatively charged state, as previously described in the Introduction.<sup>1</sup> Figure 4 shows the POM images of NLC DEDs under crossed polarizers at different pH values when the inner and outer fluids were aqueous solutions of SDS/TWEEN 80 and PAA-*b*-LCP, respectively. The resulting NLC DED will be referred to as NLC DED<sub>PAA</sub>. Below the  $\text{pK}_a$  of PAA (i.e.,  $\text{pH} = 2, 3, \text{ and } 4$ ), the POM images revealed two +1 defects at the poles of the droplet, indicating that a hybrid configuration was adopted, with P and H configurations at the outer and inner surfaces, respectively. However, above the  $\text{pK}_a$  of PAA (i.e.,  $\text{pH} \geq 5$ ), a clear Maltese-cross pattern was observed, indicating that the NLC DED adopted an H configuration at both the inner and outer surfaces. Thus, the orientation of the NLC molecules changed from P to H when the pH at the outer surface exceeded the  $\text{pK}_a$  of PAA. The formation of this H configuration above the  $\text{pK}_a$  of PAA was a result of the charged state of PAA, which generated an electric field, thus aligning the NLC perpendicular to the surface. This result is consistent with our previous data on NLC SEDs.<sup>1</sup> Thus, the defect structure of NLC DED<sub>PAA</sub> could be classified as being pH-sensitive, and as such, it provides a basis for the application of this material in biosensors, where response to variation in pH in the target analytes is necessary.

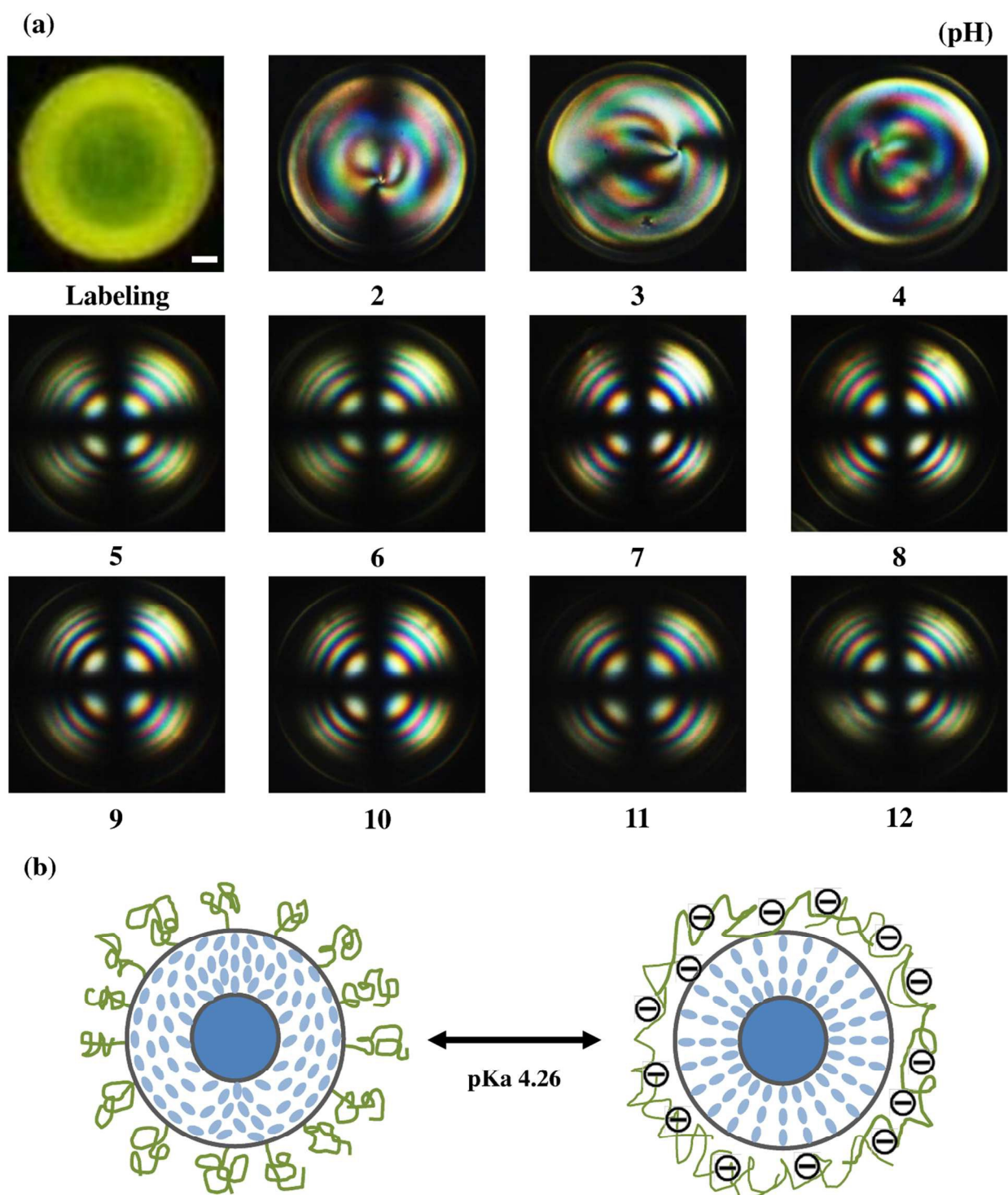


**Figure 4.** (a) POM images of the NLC  $DED_{PAA}$  at different pH values (the numbers represent the solution pH); (b) models of change in the director field of NLC  $DED_{PAA}$  at the  $pK_a$  of PAA, when the outer NLC  $DED$  surface was coated with a 0.2 wt% aqueous PAA-*b*-LCP solution and the NLC  $DED$  core was filled with a 1 wt% aqueous SDS/TWEEN 80 solution. The scale bar is

30  $\mu\text{m}$ .

**Glucose biosensor with GOx-immobilized NLC DED<sub>PAA</sub>:** GOx can be immobilized via an EDC-NHS coupling reaction. To confirm successful immobilization, the GOx was labeled with rhodamine 6G. Figure S2 shows the UV-Vis absorption spectra of GOx, GOx<sub>-rhd</sub>, and rhodamine 6G. After labeling of GOx with rhodamine 6G, the spectrum of solution<sub>GOx-Rhd</sub> (Figure S2) showed a strong characteristic rhodamine 6G peak at 520 nm, indicating that the label had been successfully attached. GOx<sub>-rhd</sub> was also immobilized on NLC DED<sub>PAA</sub> via the same EDC-NHS coupling reaction. The inset of Figure S2 shows the fluorescent image obtained upon exposure to UV light at an excitation wavelength of 365 nm. A clear green color was observed, indicating that immobilization of GOx on the NLC DED<sub>PAA</sub> surface was successful. The produced GOx-immobilized NLC DED<sub>PAA</sub> will hereafter be referred to as NLC DED<sub>PAA-GOx</sub>.

The aqueous solution in the reservoir (0.1  $\mu\text{L}$ ) was replaced with aqueous glucose solutions (0.7  $\mu\text{L}$ ) of different concentrations at pH = 7. Figure 5a shows the POM images of NLC DED<sub>PAA-GOx</sub> after addition of these glucose solutions. The initial Maltese-cross configuration (as observed in Figure 4 at pH 7) did not change upon the addition of glucose solutions at  $C_o \leq 0.08$  mM, but did change at  $C_o \geq 0.1$  mM, to give a configuration with two +1/2 defects separated at the poles. Thus, NLC DED<sub>PAA-GOx</sub> is suitable for use as a glucose biosensor, with a detection sensitivity of 0.1 mM. The initial Maltese-cross and hybrid two-defect patterns are consistent with the NLC DEDs exhibiting H/H and H/P configurations at the inner/outer surfaces in Figures 2b and 2d, respectively, indicating that the H configuration was converted to the P configuration on the outer surface. Furthermore, the H orientation at pH = 7 occurred due to deprotonation of the PAA chains, as mentioned in the previous section. As the glucose solution was introduced, an enzymatic reaction produced gluconic acid, which decreased the pH at the interface, leading to conversion to the P configuration.<sup>15</sup> Based on the observation of defect structures, we have therefore demonstrated that NLC DED<sub>PAA-GOx</sub> is capable of detecting small quantities of glucose.

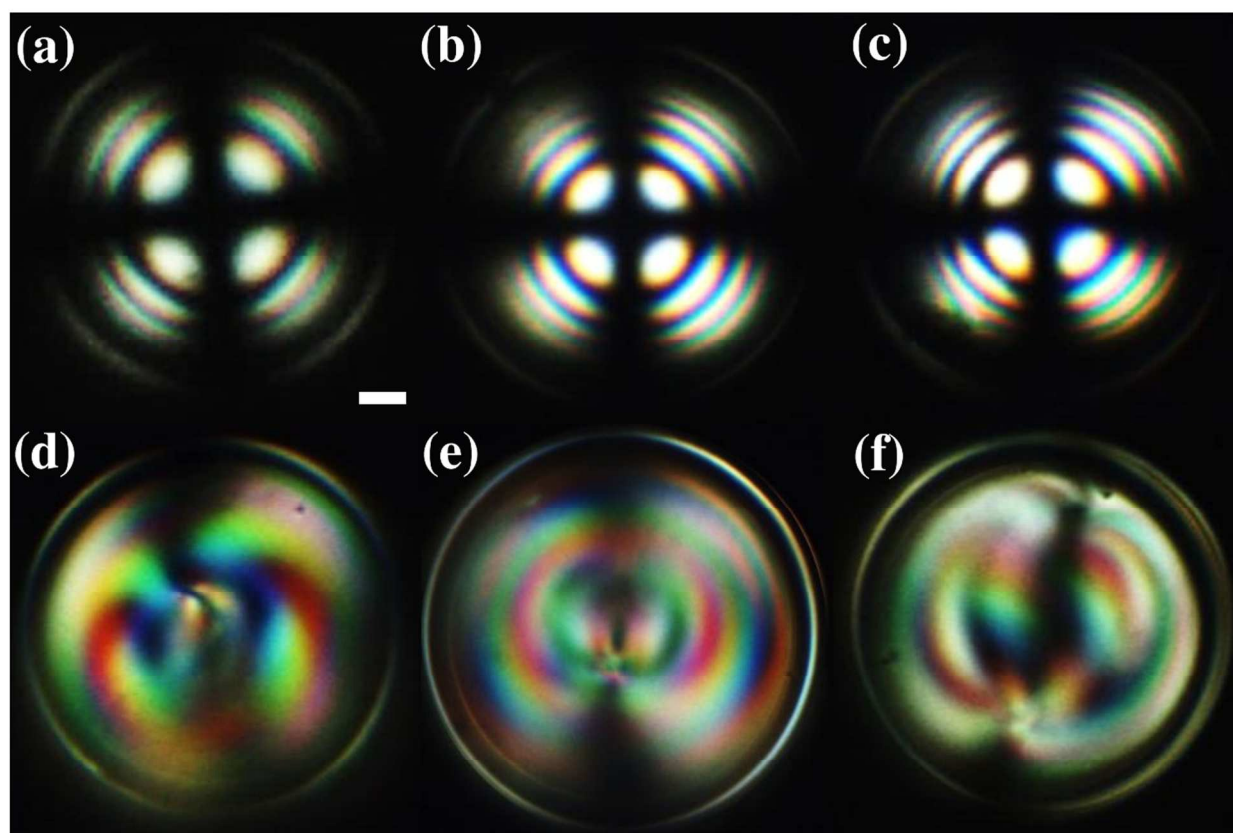


**Figure 5.** POM images of the (a) original NLC DED<sub>PAA-GOx</sub>, and original NLC DED<sub>PAA-GOx</sub> following the injection of glucose solutions at  $C_0 =$  (b) 0.05, (c) 0.08, (d) 0.1, (e) 0.5, and (f) 1 mM. The scale bar is 30  $\mu\text{m}$ .

## Conclusions

NLC DEDs were successfully produced by a microfluidic method with glass capillaries using a combined co-flow and flow-focusing geometry. Various defect structures were observed at the inner and outer surfaces when the anchoring conditions were controlled using PVA and SDS/TWEEN 80, which generated P and H configurations, respectively. Transition from the P to H configuration at the outer surface was monitored, with a change in the defect structure occurring as SDS molecules diffused to the P-configured surface. This P-to-H transition at the outer surface was also observed with NLC DED<sub>PAA</sub> when the pH exceeded the pK<sub>a</sub> of PAA. This result demonstrated that NLC DED<sub>PAA</sub> was pH-responsive. Furthermore, the pH responsiveness of the NLC DED<sub>PAA</sub> defect structure was employed for glucose biosensor by immobilizing GOx on the PAA. We have therefore demonstrated that NLC DEDs can be successfully coated with a pH-responsive polyelectrolyte block copolymer, potentially allowing the formation of a broad range of polyelectrolyte-functionalized NLC DEDs for LC-based biosensors.

## Acknowledgements

This work was supported by the National Research Foundation of Korea (NRF-2011-0020264 and NRF-2014R1A2A1A11050451).

## Notes and references

Electronic Supplementary Information (ESI) available: Experimental details, scheme, figures and video of this work.

1. W. Khan, J. H. Choi, G. M. Kim and S.-Y. Park, *Lab on a Chip*, 2011, **11**, 3493-3498.
2. J. M. Brake, M. K. Daschner, Y.-Y. Luk and N. L. Abbott, *Science*, 2003, **302**, 2094-2097.
3. W. Khan and S.-Y. Park, *Lab on a Chip*, 2012, **12**, 4553-4559.
4. T. Bera, J. Deng and J. Fang, *The Journal of Physical Chemistry B*, 2014, **118**, 4970-4975.
5. J.-S. Park and N. L. Abbott, *Advanced Materials*, 2008, **20**, 1185-1190.
6. J. M. Brake, A. D. Mezera and N. L. Abbott, *Langmuir*, 2003, **19**, 6436-6442.
7. J. Zou, T. Bera, A. A. Davis, W. Liang and J. Fang, *The Journal of Physical Chemistry B*, 2011, **115**, 8970-8974.
8. J.-M. Seo, W. Khan and S.-Y. Park, *Soft Matter*, 2012, **8**, 198-203.
9. M. Omer, M. Islam, M. Khan, Y. Kim, J. Lee, I.-K. Kang and S.-Y. Park, *Macromol. Res.*, 2014, **22**, 888-894.
10. M. I. Kinsinger, B. Sun, N. L. Abbott and D. M. Lynn, *Advanced Materials*, 2007, **19**, 4208-4212.
11. D.-Y. Lee, J.-M. Seo, W. Khan, J. A. Kornfield, Z. Kurji and S.-Y. Park, *Soft Matter*, 2010, **6**, 1964-1970.
12. H.-L. Liang, R. Zentel, P. Rudquist and J. Lagerwall, *Soft Matter*, 2012, **8**, 5443-5450.
13. M. Omer and S.-Y. Park, *Anal Bioanal Chem*, 2014, **406**, 5369-5378.
14. M. Omer, M. Khan, Y. K. Kim, J. H. Lee, I. K. Kang and S. Y. Park, *Colloids and surfaces. B, Biointerfaces*, 2014, **121**, 400-408.
15. J. Kim, M. Khan and S.-Y. Park, *ACS Applied Materials & Interfaces*, 2013, **5**, 13135-13139.
16. S. Munir, M. Khan and S.-Y. Park, *Sensors and Actuators B: Chemical*, 2015, **220**, 508-515.
17. M. Khan and S.-Y. Park, *Sensors and Actuators B: Chemical*, 2014, **202**, 516-522.
18. D. R. Nelson, *Nano Letters*, 2002, **2**, 1125-1129.
19. A. Fernández-Nieves, V. Vitelli, A. S. Utada, D. R. Link, M. Márquez, D. R. Nelson and D. A. Weitz, *Physical Review Letters*, 2007, **99**, 157801.
20. A. S. Utada, E. Lenceau, D. R. Link, P. D. Kaplan, H. A. Stone and D. A. Weitz, *Science*, 2005, **308**, 537-541.

21. H.-L. Liang, J. Noh, R. Zentel, P. Rudquist and J. P. F. Lagerwall, *Philosophical Transactions of the Royal Society of London A: Mathematical, Physical and Engineering Sciences*, 2013, **371**.
22. A. A. Sonin, *The Surface Physics of Liquid Crystals*, Gordon and Breach Publishers, 1995.
23. J. Jiao and D. Burgess, *AAPS PharmSci*, 2003, **5**, 62-73.
24. T. Lopez-Leon and A. Fernande-Nieves, *Physical Review E*, 2009, **79**, 021707.

### Table of contents

The glucose was detected successfully by the configuration change of the glucose oxidase (GOx)-immobilized NLC DED<sub>PAA</sub> through enzymatic reaction.

